

Weierstraß-Institut
für Angewandte Analysis und Stochastik
Leibniz-Institut im Forschungsverbund Berlin e. V.

Preprint

ISSN 2198-5855

**A multi-mode delay differential equation model for lasers with
optical feedback**

Mindaugas Radziunas

submitted: 6 September 2016

Weierstrass Institute
Mohrenstr. 39
10117 Berlin
Germany
E-Mail: mindaugas.radziunas@wias-berlin.de

No. 2294
Berlin 2016



2010 *Mathematics Subject Classification.* 78A60 78M34 35L40 58D30.

2008 *Physics and Astronomy Classification Scheme.* 42.55.Px 42.60.-v 02.30.Jr 02.30.Ks.

Key words and phrases. lasers, external cavity, optical feedback, cavity mode, modeling, traveling wave, Lang Kobayashi, multi-mode, delay differential equations.

Edited by
Weierstraß-Institut für Angewandte Analysis und Stochastik (WIAS)
Leibniz-Institut im Forschungsverbund Berlin e. V.
Mohrenstraße 39
10117 Berlin
Germany

Fax: +49 30 20372-303
E-Mail: preprint@wias-berlin.de
World Wide Web: <http://www.wias-berlin.de/>

Abstract

In this paper, we discuss the relations between the spatially-distributed traveling wave, Lang-Kobayashi, and a new multi-mode delay differential equation models for Fabry-Perot type semiconductor diode lasers with an external optical feedback. All these models govern the dynamics of the slowly varying complex amplitudes of the optical fields and carrier density. To compare the models, we calculate the cavity modes determined by the threshold carrier density and optical frequency of the steady states in all three models. These calculations show that the Lang-Kobayashi type model is in good agreement with the traveling wave model only for the small feedback regimes, whereas newly derived multi-mode delay differential equation model remains correct even at moderate and large optical feedback regimes.

1 Introduction

In this work, we consider and compare three models describing nonlinear dynamics of complex slowly varying amplitudes of optical fields E and carrier densities n in the Fabry-Perot type diode laser with an optical feedback from the external cavity (EC), see Fig. 1(a). Our general approach is given by the traveling wave (TW) model, which is a 1(space)+1(time) dimensional system of partial differential equations describing the longitudinal and temporal evolution of counter-propagating optical fields, E_+ and E_- , and dynamics of spatially averaged carrier density [1]. Another approach is a well-known delay differential equation (DDE) model of Lang-Kobayashi (LK) type, which was originally used for investigation of dynamics in single-mode lasers with *long* ECs and *weak* optical feedback [2]. The last multi-mode (MM) model proposed in this work is also given by a system of DDEs for optical fields and carriers. Similarly to DDE model for mode-locked lasers reported in [3, 4, 5], it is derived from the TW model under assumptions of ring configuration of the diode laser and unidirectional propagation of the optical field within this ring, see Fig. 1(b). In contrast to the LK type models, this MMDDE model properly accounts for multiple longitudinal modes of the diode laser and, therefore, admits considering *moderate* and *strong* optical feedback regimes. Such kind of feedback is typical for a large class of external cavity diode lasers, where the optical length of the EC is comparable to the diode length [6], whereas the field reflectivity at the rear facet of the diode is reduced, such that the solitary lasing can be achieved only at very high bias currents. On the other hand, comparing to the TW model, our new MMDDE model is relatively simple and admits fast numerical integration, numerical bifurcation analysis [7], and more detailed analytic investigations.

In all three cases, we assume that the action of the EC, i.e., the relation between the optical field $F_i(t)$ reinjected into the diode and the field $F_e(t)$ emitted from the diode is given by the linear operator \mathcal{F} . For the simple EC determined by an external mirror, \mathcal{F} is a simple time-delay operator:

$$F_i(t) = [\mathcal{F}F_e](t) = Ke^{i\phi}F_e(t-\tau), \quad (1)$$

where τ is the field roundtrip time in the EC, whereas K and ϕ are the transmission factor and the phase shift of the complex field amplitude during this roundtrip. More sophisticated

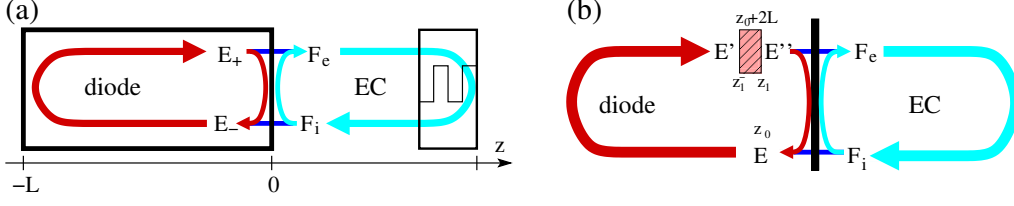


Figure 1: Schematic representations of the diode laser with the external cavity. (a): linear configuration, as considered in the TW model. (b): ring diode laser configuration (left) with a localized filtering element (hatched box) and the filtered optical feedback from the external cavity (right), as considered in the new MMDDE model.

ECs can contain several reflectors [8] or different frequency filtering elements, such as passive resonators [9] or Bragg gratings [6]. In the mirror or resonator case, \mathcal{F} still can be represented explicitly as a linear combination of a finite or an infinite number of time delay operators with multiple delays. For distributed reflectors (Bragg gratings), the required value of F_i can be found integrating numerically an additional set of *mutually coupled* TW field equations within this filtering element [10]. Alternatively, one can approximate the action of various objects of the EC by linear continuous time filters described by ODEs. For example, the delay operator (1) can be interpreted as a broad Lorentzian filter,

$$\begin{aligned} F_i(t) &= [\mathcal{F}F_e](t) = \tilde{\gamma} K e^{i\phi} \int_{-\infty}^{t-\tau} e^{-\tilde{\gamma}(t-\tau-\nu)} F_e(\nu) d\nu \\ \Rightarrow \frac{1}{\tilde{\gamma}} \frac{d}{dt} F_i(t) &= K e^{i\phi} F_e(t-\tau) - F_i(t), \end{aligned} \quad (2)$$

in the limit case of $\tilde{\gamma} \rightarrow +\infty$. Note, that such kind of filter we also use for modeling of material gain dispersion in the TW model (3).

For the sake of simplicity, we consider only the simplest case of the EC determined by Eq. (1) or Eq. (2) in this work. Below we formulate the normalized TW, LK, and MMDDE models, discuss the relations of the model parameters, compare optical frequencies and threshold carrier densities of the steady states of all models in weak, moderate and strong feedback regimes, and, finally, compare trajectories obtained by direct numerical integration of the presented models.

2 Traveling wave model

After a suitable normalization [11], the spatially-distributed TW model within the laser diode can be written as

$$\begin{aligned} (\partial_t \pm \partial_z) E_{\pm} &= \left((1 + i\alpha_H) n - \frac{\xi_0}{L} - \mathcal{P} \right) E_{\pm}, \\ \mathcal{P} E_{\pm} &= \frac{\bar{g}}{2} (E_{\pm} - P_{\pm}), \quad \frac{d}{dt} P_{\pm} = \bar{\gamma} E_{\pm} + (i\bar{\omega} - \bar{\gamma}) P_{\pm}, \\ \epsilon^{-1} \frac{d}{dt} n &= J - n - \Re \langle (E, [2n + 1 - 2\mathcal{P}] E) \rangle. \end{aligned} \quad (3)$$

Here, the dimensionless spatial coordinate, $z \in (-L, 0)$, is the longitudinal position along the Fabry-Perot type laser diode multiplied with the threshold gain of the solitary laser, see Fig. 1(a). The scaled time coordinate t is such that the field propagation time along the diode is L . The linear operator \mathcal{P} and the polarization functions P_{\pm} model the Lorentzian approximation of the material gain dispersion with \bar{g} , $\bar{\omega}$, and $\bar{\gamma}$ denoting its amplitude, peak frequency

detuning from the central frequency, and the half width at the half maximum [1]. $\langle(\xi, \zeta)\rangle = \frac{1}{L} \int_{-L}^0 (\xi(z), \zeta(z)) dz$ is the spatial average of the standard inner product of the vectors ξ and ζ , $(\xi, \zeta) = \xi_+^* \zeta_+ + \xi_-^* \zeta_-$, $|E(z, t)|^2 = (E, E)$ is the longitudinal distribution of the scaled local photon density, and n is the spatially averaged excess carrier density. Parameters α_H and J are the linewidth enhancement factor and the excess carrier injection, whereas ϵ represents the ratio of the photon and carrier lifetimes. The complex factor ξ_0 is determined by the relation $e^{2\xi_0} = -r_f^* r_r e^{-2\chi(0)}$, where r_f and r_r are complex field amplitude reflection coefficients at the front ($z = -L$) and rear ($z = 0$) diode facets, whereas $\chi(\omega) = \frac{\bar{g}L}{2} \frac{i(\omega - \bar{\omega})}{\bar{\gamma} + i(\omega - \bar{\omega})}$. To complete the model equations, we define the following field reflection-transmission-reinjection conditions at the diode facets:

$$E_+(-L, t) = -r_f^* E_-(-L, t), \quad \begin{pmatrix} F_e(t) \\ E_-(0, t) \end{pmatrix} = \begin{pmatrix} t_r & -r_r^* \\ r_r & t_r \end{pmatrix} \begin{pmatrix} E_+(0, t) \\ F_i(t) \end{pmatrix}, \quad (4)$$

where $t_r = \sqrt{1 - |r_r|^2}$ is the field amplitude transmission through the rear facet, whereas $F_e(t)$ and $F_i(t)$ are related by Eq. (1).

Assume that for a fixed carrier number $n(t) = \bar{n}$ the field functions are monochromatic waves with the optical frequency ω . Namely, $E_{\pm}(z, t) = \hat{E}_{\pm}(z) e^{i\omega t}$, $P_{\pm}(z, t) = \hat{P}_{\pm}(z) e^{i\omega t}$, and $F_{e,i}(t) = \hat{F}_{e,i} e^{i\omega t}$. By substituting these expressions into Eqs. (1), (3), (4) and resolving the resulting ODEs within the diode, one gets the following relations of the emission and reinjection factors \hat{F}_e and \hat{F}_i :

$$\begin{aligned} \hat{F}_i &= \mathcal{R}(\omega) \hat{F}_e, \quad \mathcal{R}(\omega) = K e^{i\phi} e^{-i\omega\tau}, \\ \hat{F}_e &= \mathcal{G}_{TW}(\bar{n}, \omega) \hat{F}_i, \quad \mathcal{G}_{TW}(\omega) = \frac{|r_r|^2 e^{2\xi(\bar{n}, \omega) - \mathcal{D}_{TW}(\omega)}}{r_r (\mathcal{D}_{TW}(\omega) - e^{2\xi(\bar{n}, \omega)})}, \\ \xi &= [i\omega - (1 + i\alpha_H)\bar{n}]L, \quad \mathcal{D}_{TW}(\omega) = e^{2(\chi(0) - \chi(\omega))}. \end{aligned} \quad (5)$$

Function \mathcal{R} is a frequency domain representation of the operator \mathcal{F} and shows the response of the EC to the incoming monochromatic field. In the considered simple example, $|\mathcal{R}(\omega)| = K$ for any frequency ω . Functions \mathcal{D}_{TW} and \mathcal{G}_{TW} represent an impact of the material gain dispersion and the response of the diode to the incoming monochromatic field at fixed \bar{n} , respectively. Due to the special normalization of carriers and choice of $\Im\xi_0$, the solitary laser has a steady state with $(\bar{n}, \omega) = (0, 0)$ and, therefore, $\mathcal{G}_{TW}^{-1}(0, 0) = 0$. After neglecting gain dispersion ($\mathcal{D}_{TW} \equiv 1$), one can rewrite this function in the vicinity of $(0, 0)$ as $\mathcal{G}_{TW}^{-1}(\bar{n}, \omega) = \frac{2r_r}{i\bar{\gamma}} \xi(\bar{n}, \omega) + \mathcal{O}(|\xi|^2)$.

An elimination of the factors \hat{F}_e and \hat{F}_i in Eqs. (5) imply a complex characteristic equation $\mathcal{G}_{TW}^{-1}(\bar{n}, \omega) = \mathcal{R}(\omega)$ for two real numbers \bar{n} and ω determining all possible steady states (or compound cavity modes, CCMs) of the TW model [11], see, e.g., large full bullets in Fig. 2. These CCMs play the same role as the external cavity modes (ECMs) of the LK type models (small full bullets in the same figure). In our case of the simple EC, all these modes are located on the set of thick gray curves, which are determined by the real equation $K = |\mathcal{G}_{TW}^{-1}(\bar{n}, \omega)|$. The curves are parametrized by the phase factor ϕ , and are similar to the ‘‘ellipses of the ECMs’’ of the LK model (thin solid curves in the same figure).

3 Lang-Kobayashi type model

The normalized LK type model can be written as

$$\begin{aligned} \frac{d}{dt}E &= (1+i\alpha_H)nE + CF_i, \quad F_i(t) = [\mathcal{F}E](t), \\ \epsilon^{-1}\frac{d}{dt}n &= J - n - (2n+1)|E|^2, \end{aligned} \quad (6)$$

where the operator \mathcal{F} and parameters J, ϵ and α_H are the same as in the TW model discussed above. The coefficient C relates the feedback *rate* (which in the unscaled LK model would have the dimension s^{-1}) with the dimensionless field transmission factor $Ke^{i\phi}$ from (1).

Similarly to above considered TW model case, the assumption $n(t) = \bar{n}$ and the substitution of $E = F_e = \hat{E}e^{i\omega t}$ and $F_i = \hat{F}_i e^{i\omega t}$ into Eqs. (1,6) imply the complex equation $\frac{1}{CL}\xi(\bar{n}, \omega) = \mathcal{R}(\omega)$ determining ECMs (\bar{n}, ω) of the LK model. It is clear that an agreement between the CCMs of the TW model and ECMs of the LK model can be achieved, if $\frac{1}{CL}\xi(\bar{n}, \omega) \approx \mathcal{G}_{TW}^{-1}(\bar{n}, \omega)$. In the vicinity of $(\bar{n}, \omega) = (0, 0)$, this condition is accomplished by adjusting $C = \frac{t_r^2}{2r_r L}$. For more details see [11].

4 Multi-mode DDE model

Following Ref. [3], we neglect back propagating field E_- in the TW model, assume the ring configuration of the diode laser, such that the longitudinal coordinates z_0 and $z_1 = z_0 + 2L$ correspond to the same position on the ring, concentrate all accumulated distributed field amplitude losses, frequency detuning, and field dispersion within the diode at the interval of vanishing length, $[z_1^-, z_1]$, [hatched box in Fig. 1(b)], and allow the spatial distribution of carriers. The resulting TW model within (z_0, z_1^-) reads as

$$\begin{aligned} (\partial_t + \partial_z) E_+(z, t) &= \frac{(1+i\alpha_H)}{2}[2n(z, t) + 1]E_+(z, t), \\ \epsilon^{-1}\partial_t n(z, t) &= J - n(z, t) - [2n(z, t) + 1]|E_+(z, t)|^2. \end{aligned}$$

The relation

$$\begin{aligned} E''(t) &= (\gamma' - i\bar{\omega})\mu \int_{-\infty}^{t-\Delta} e^{(i\bar{\omega}-\gamma')(t-\Delta-\nu)} E'(\nu) d\nu \\ \Rightarrow \frac{d}{dt}E''(t) &= (\gamma' - i\bar{\omega})(\mu E'(t-\Delta) - E''(t)) \end{aligned}$$

at the point-filtering element connects the incident and transmitted fields $E'(t) = E_+(z_1^-, t)$ and $E''(t) = E_+(z_1, t)$. Here, $\gamma' = \frac{\tilde{\gamma}}{\sqrt{2g}L}$ and $\mu = r_r^{-1}e^{-(1+i\alpha_H)L}$ represent the filter bandwidth and accumulated losses/detuning, whereas $\Delta = \frac{gL - \sqrt{2g}L}{\tilde{\gamma}}$ is a finite filter response time, $\Delta \ll 2L$, such that the effective round trip time in the diode is $\tau_d = 2L + \Delta$. The action of the EC is given by Eq. (2) with $\tilde{\gamma} \gg 1$, whereas the optical fields at the interface of the diode and the EC, see Fig. 1(b), are related by the field reflection-transmission condition (4) with $E^+(0, t)$ and $E^-(0, t)$ substituted by $E''(t)$ and $E(t) = E_+(z_0, t)$, respectively. After introducing the notation for forward along the characteristic line $t - z = \text{const}$ performed sliding average of the carrier density, $\tilde{n}(t) = \frac{1}{2L} \int_{z_0}^{z_1} n(\nu, t + \nu - z_0) d\nu$, and resolving the unidirectional TW model presented above one can obtain [3] the carrier rate equation

$$\epsilon^{-1}\frac{d}{dt}\tilde{n} = J - \tilde{n} - \frac{1}{2L} [e^{[2\tilde{n}+1]2L} - 1] |E|^2, \quad (7)$$

and the relation $E'(t+2L) = e^{(1+i\alpha_H)[2\tilde{n}(t)+1]L} E(t)$ between the field functions E and E' . All together, all these relations of the carrier function \tilde{n} and the field functions $E, E', E'', F_e,$ and F_i is a system of algebro-differential equations with a time delay. The elimination of $E', E'', F_e,$ and introduction of the new variable $F = \frac{1}{t_r} F_i$ imply the following couple of the field equations,

$$\begin{aligned} \frac{d}{dt} E &= -(\gamma' - i\bar{\omega})E(t) + t_r^2 (\gamma' - i\bar{\omega} - \tilde{\gamma})F(t) + t_r^2 \frac{\tilde{\gamma} K e^{i\phi}}{r_r} (E(t - \tau) - F(t - \tau)) \\ &\quad + (\gamma' - i\bar{\omega}) e^{(1+i\alpha_H)\tilde{n}(t-\tau_d)2L} E(t - \tau_d), \\ \frac{d}{dt} F &= -\tilde{\gamma} F(t) + \frac{\tilde{\gamma} K e^{i\phi}}{r_r} (E(t - \tau) - F(t - \tau)), \end{aligned} \quad (8)$$

which, together with the carrier rate equation (7), complete out new multi-mode DDE model for lasers with an external feedback. It is noteworthy, that the field function $E(t)$ in the MMDDE model represents an incident optical field at the rear side of the diode, whereas the field at the front facet of the diode is given by $E(t) e^{\frac{1+\alpha_H}{2}(2\tilde{n}(t-L)+1)L}$.

The assumption $\tilde{n}(t) = \bar{n}$ and the relations between the frequency domain representations of the optical fields give rise to the following EC and diode response functions:

$$\begin{aligned} \mathcal{R}_{MM}(\omega) &= \frac{\hat{F}_i}{\hat{F}_e} = K e^{i\phi} e^{-i\omega\tau} [1 + i\frac{\omega}{\tilde{\gamma}}]^{-1} = \mathcal{R}(\omega) + \mathcal{O}(\frac{\omega}{\tilde{\gamma}}), \\ \mathcal{G}_{MM}(\bar{n}, \omega) &= \frac{\hat{F}_e}{\hat{F}_i} = \frac{|r_r|^2 e^{2\xi(\bar{n}, \omega)} - \mathcal{D}_{MM}(\omega)}{r_r (\mathcal{D}_{MM}(\omega) - e^{2\xi(\bar{n}, \omega)}), \quad \text{where} \\ \mathcal{D}_{MM} &= \frac{(\gamma' - i\bar{\omega}) e^{-i\omega\Delta}}{\gamma' + i(\omega - \bar{\omega})} = \mathcal{D}_{TW} (1 + \mathcal{O}(\frac{\bar{\omega}^2 + \omega^2}{\tilde{\gamma}^2})). \end{aligned}$$

The form of the function \mathcal{G}_{TW} in (5) and the expressions above show that for $\tilde{\gamma} \rightarrow +\infty$ and $\tilde{\gamma} \gg |\omega| + |\bar{\omega}|$ the diode and EC responses in the TW model are well approximated by the corresponding functions of the new modeling approach independently on the feedback factor K . This approximation is also illustrated by nearly coinciding cavity mode curves of the MMDDE (thin dashed) and TWE (thick gray) models in Fig. 2.

5 Comparison of the models

First of all, to analyze the agreement of three modeling approaches, we compare cavity modes (CMs) which are the steady states of the corresponding system and are defined by the threshold carrier number \bar{n} and the relative optical frequency ω . The choice of the scaling factor C in the LK model [11] and the parameters γ', μ, Δ in the MMDDE model provide the best fitting of the CMs in the reduced DDE models to the CMs of the TW model. To find the CMs and to draw the cavity mode curves for varying feedback phase parameter ϕ , we consider a 2 mm long diode laser with the 16.2 mm long EC. The parameters of the field equations in the normalized models are $L = 3, \alpha_H = 1.2, \tau = 13.5, \tilde{\gamma} = 500, r_f = \sqrt{0.3}, r_r = e^{-2.84}/r_f \approx 0.1, \bar{\omega} = 0, \bar{g} = 6, \tilde{\gamma} = 120$, s.t. $\gamma' = 20, \Delta = 0.1$, and $\tau_d = 6.1$.

The curves in Fig. 2 represent all possible locations of the CMs for fixed feedback amplitude factor K and arbitrary feedback phase ϕ . For small K , the CMs of the LK model provide a good approximation of the CMs of the TW model in the vicinity of the origin $(\omega, \bar{n}) = (0, 0)$, see thin dark and thick gray solid curves within the insert of Fig. 2. We note, however, that for small K and fixed ϕ , the LK model has a unique CM (full bullet in Fig. 2 at $K = 0.02$), whereas

the TW model has multiple CMs with similar separation ($\sim \pi/L$) of mode frequencies ω and similar thresholds \bar{n} (large red bullets in the same figure). For moderate and large feedback, $K = 0.2$ and $K = 0.5$, the agreement between the LK and TW equations is drastically degraded: whereas the CMs of the LK model are located on the increasing ellipses centered at the origin $(0, 0)$, the CMs of the TW model are on a single, only slightly undulated nearly horizontal non-connected curve. In contrast, the CMs of our new MMDDE model are in perfect agreement with the CMs of the TW model for all values of K : see indistinguishable thin dashed and thick gray curves in Fig. 2.

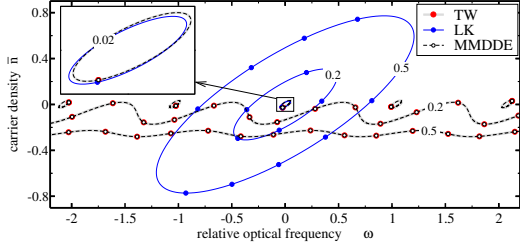


Figure 2: Locations of cavity modes in the TW (thick grey), LK (thin solid) and MMDDE (thin dashed) models for $K = 0.02$, $K = 0.2$, and $K = 0.5$. Other parameters are defined in Section 5. Bullets on the corresponding curves show the location of the CMs for fixed phase factor, $\phi = 0$. An insert shows enlarged curves for $K = 0.02$ in the vicinity of the origin.

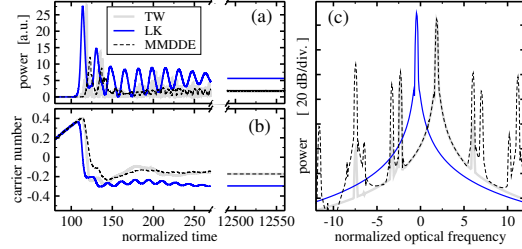


Figure 3: Simulated switching on of the external cavity laser in the TW (thick gray), LK (thin solid) and MMDDE (thin dashed) models. Parameters $\epsilon = 4 \cdot 10^{-3}$, $J = 2$, $K = 0.2$, and $\phi = \pi/2$. (a) and (b): timetraces of the scaled emitted power and excess carrier number. (c): optical spectra estimated after $T = 1250$ transient simulations.

To check the dynamical performance of all considered models, we have also simulated switching on of the external cavity laser in the moderate feedback ($K = 0.2$, $\phi = \pi/2$) and carrier injection ($J = 2$) regime. The results of simulations are shown in Fig. 3. Optical fields and carrier number shown in panels (a) and (b) of this figure represent a typical laser switching behavior in all three models. In all three cases, a long enough transient simulations lead to one of the available steady states determined by the CMs. Due to a significant difference of the CM thresholds in the LK and TW or MMDDE models at the considered moderate feedback level, the switching in the LK model occurs slightly earlier, and the corresponding carrier number of the final steady state is significantly smaller than that one of the steady states in the TW and MMDDE models, see panel (b) of Fig. 3. Panel (c) of the same figure represents optical spectra of the transient complex optical fields. Here again, we can see discrepancies between the operating frequencies calculated according to the LK (thin solid) and TW or MMDDE (thick gray or thin dashed) models. Whereas the optical spectra due to the LK model has a single line determined by the minimal threshold (maximal gain) mode, the spectra obtained using the TW and MMDDE models have multiple lines corresponding to the location of the adjacent CMs and various mixing products of these modes. We also note that this figure shows some differences between the general TW and newly derived MMDDE models. Namely, the difference of the side peaks in the corresponding optical spectra indicate a weaker side mode suppression in the MMDDE model. The stability properties of the CMs, however, will be studied in subsequent

papers.

In conclusion, we present a new multi-mode delay differential equation model for studying dynamics in external cavity diode lasers. Even though a similar model has been used already for a study of coupled cavity mode-locked lasers, the present work gives a correct relation of the MMDDE to the original TW model and proposes to use this new model for a general class of external cavity diode lasers.

References

- [1] U. Bandelow, M.R.J. Sieber, M. Wolfrum, *IEEE J. of Quantum Electronics* **37**, 183 (2001)
- [2] R. Lang, K. Kobayashi, *IEEE J. of Quantum Electronics* **16**, 347 (1980)
- [3] A.G. Vladimirov, D. Turaev, *Phys. Rev. A* **72**, 033808 (2005)
- [4] R.M. Arkhipov, A. Amann, A.G. Vladimirov, *Appl. Phys. B* **118**, 539 (2015)
- [5] L. Jaurigue, A. Pimenov, D. Rachinskii, E. Schöll, K. Lüdge, A. Vladimirov, *Phys. Rev. A* **92**(5), 053807 (2015)
- [6] M. Radziunas, V.Z. Tronciu, C. Kürbis, H. Wenzel, A. Wicht, *IEEE J. of Quantum Electronics* **51**, 2000408 (2015)
- [7] K. Engelborghs, T. Luzyanina, G. Samaey, DDE-BIFTOOL v. 2.00: a Matlab package for bifurcation analysis of delay differential equations. Tech. Rep. TW330, Katholieke Universiteit Leuven, Belgium (2001)
- [8] V.Z. Tronciu, C.R. Mirasso, P. Colet, M. Hamacher, M. Benedetti, V. Vercesi, V. Annovazzi-Lodi, *IEEE J. of Quantum Electronics* **46**, 1840 (2011)
- [9] S. Schikora, H.J. Wünsche, F. Henneberger, *Phys. Rev. E* **83**, 026203 (2011)
- [10] J.E. Carroll, J. Whiteaway, D. Plumb, *Distributed feedback semiconductor lasers* (IEE, London, 1998)
- [11] M. Radziunas, H.J. Wünsche, B. Krauskopf, M. Wolfrum, in *SPIE Proceedings Series*, vol. 6184 (2006), vol. 6184, p. 61840X